



HAL
open science

Upregulation of c-mip is closely related to podocyte dysfunction in membranous nephropathy.

Kelhia Sendeyo, Vincent Audard, Shao-Yu Zhang, Qingfeng Fan, Khedidja Bouachi, Mario Ollero, Catherine Rucker-Martin, Elodie Gouadon, Dominique Desvaux, Franck Bridoux, et al.

► To cite this version:

Kelhia Sendeyo, Vincent Audard, Shao-Yu Zhang, Qingfeng Fan, Khedidja Bouachi, et al.. Upregulation of c-mip is closely related to podocyte dysfunction in membranous nephropathy.. *Kidney International*, 2013, 83 (3), pp.414-25. 10.1038/ki.2012.426 . inserm-00815234

HAL Id: inserm-00815234

<https://inserm.hal.science/inserm-00815234>

Submitted on 18 Jul 2013

HAL is a multi-disciplinary open access archive for the deposit and dissemination of scientific research documents, whether they are published or not. The documents may come from teaching and research institutions in France or abroad, or from public or private research centers.

L'archive ouverte pluridisciplinaire **HAL**, est destinée au dépôt et à la diffusion de documents scientifiques de niveau recherche, publiés ou non, émanant des établissements d'enseignement et de recherche français ou étrangers, des laboratoires publics ou privés.



Upregulation of c-mip precedes podocyte dysfunction in membranous nephropathy

Journal:	<i>Kidney International</i>
Manuscript ID:	KI-04-12-0598.R2
Manuscript Type:	Original Article-Basic Research
Date Submitted by the Author:	26-Sep-2012
Complete List of Authors:	Sendeyo, kélhia; AP-HP, cell biology Audard, vincent; AP-HP, Henri Mondor Hospital, nephrology Zhang, Shao-yu; INSERM, UMR 955, Fan, qingfeng; INSERM U955, cell biology Bouachi, Khedidja; INSERM, UMR 955, Ollero, Mario; INSERM, UMR 955, cell biology Gouadon, Elodie; INSERM UMR-S 999, Centre Chirurgical Marie Lannelongue Desvaux, Dominique; AP-HP, Henri Mondor Hospital, Histology Rucker, Catherine; INSERM UMR-S 999, Centre Chirurgical Marie Lannelongue Bridoux, Franck; CHU Poitiers, nephrology Guellaën, Georges; INSERM, UMR 955, Ronco, Pierre; Université Pierre et Marie Curie-Paris 6, INSERM UMRS-702 Lang, philippe; INSERM, UMR 955, Pawlak, andre; INSERM, UMR 955, Sahali, Djilalli; INSERM, UMR 955,
Subject Area:	Renal Pathology , Immunology , Cell Biology
Keywords:	glomerular disease, Heymann nephritis, membranous nephropathy, nephrotic syndrome, Pathophysiology of Renal Disease and Progression

SCHOLARONE™
Manuscripts

Upregulation of c-mip is closely related to podocyte dysfunction in membranous nephropathy

Kelhia Sendeyo^{1,2*}, Vincent Audard^{1,2,3*}, Shao-yu Zhang^{1,2,3*}, Qingfeng Fan^{1,2}, Khedidja Bouachi^{1,2,3}, Mario Ollero^{1,2}, Catherine Rucker-Martin^{4,5}, Elodie Gouadon^{4,5}, Dominique Desvieux^{1,2,6}, Franck Bridoux⁷, Georges Guellaën^{1,2}, Pierre Ronco^{8,9}, Philippe Lang^{1,2,3,10}, Andre Pawlak^{1,2} and Djillali Sahali^{1,2,3,10,11}

¹INSERM, U 955, Equipe 21, F-94010, Créteil, France.

²Université Paris-Est Créteil Val-de-Marne, F-94010, Créteil, France.

³AP-HP, Groupe hospitalier Henri Mondor-Albert Chenevier, Service de Néphrologie, F-94010, Créteil, France.

⁴Centre Chirurgical Marie Lannelongue, INSERM UMR-S 999, LabEx LERMIT, F-92350, Le Plessis Robinson, France.

⁵Université Paris-Sud, Faculté de médecine, F-94275, Le Kremlin-Bicêtre, France.

⁶Assistance publique-Hôpitaux de Paris (AP-HP), Groupe hospitalier Henri Mondor-Albert Chenevier, Département de Pathologie, F-94010, Créteil, France.

⁷Service de Néphrologie, Hémodialyse et Transplantation Rénale, Hôpital Jean Bernard, CHU Poitiers, 86021 Poitiers, France.

⁸INSERM UMRS-702, F-75020 Paris, France.

⁹Université Pierre et Marie Curie-Paris 6; 75252 Paris Cedex 05, France.

¹⁰Institut francilien de recherche en néphrologie et transplantation, Henri Mondor, F-94010, France.

*KS, VA and SYZ are equally contributed for this work

VA is a recipient of an INSERM Poste d'Accueil (Institut National de la Santé et de la Recherche Médicale)

¹¹Address correspondence to : Dil Sahali, INSERM, U 955. Tel : 33149812537 ; Fax : 33149812539 ; email : dil.sahali@inserm.fr

This work was supported in part by an Avenir Program from INSERM, a grant from the French Kidney Foundation and Association pour l'Utilisation du Rein Artificiel (AURA).

The authors have declared that no conflict of interest exists

1
2
3
4
5
6
7
8
9
10
11
12
13
14
15
16
17
18
19
20
21
22
23
24
25
26
27
28
29
30
31
32
33
34
35
36
37
38
39
40
41
42
43
44
45
46
47
48
49
50
51
52
53
54
55
56
57
58
59
60

For Peer Review Only

Abstract

Membranous nephropathy (MN) is a glomerular disease characterized by a nephrotic syndrome without infiltration of inflammatory cells or proliferation of resident cells. Although the cause of the disease is unknown, the primary pathogenic mechanism responsible for the accumulation of immune deposits on the outer aspect of the glomerular basement membrane involves the generation of autoantibodies against antigen targets expressed at the membrane surface of podocyte. The molecular mechanisms of nephrotic proteinuria, which reflects a profound disorder of podocyte function, remain unclear. We show here that induction of c-mip in passive type Heymann nephritis (PHN) coincides with the occurrence of proteinuria. c-mip expression is not detectable in the glomeruli of PHN rats receiving a single dose of anti-megalin polyclonal antibody, yet the immune complexes are readily present but without triggering of proteinuria. Rats reinjected with anti-megalin develop a few days later heavy proteinuria concomitantly with c-mip overproduction in podocytes. We show that overexpression of c-mip is associated with downregulation of synaptopodin in human MN, PHN rats and c-mip transgenic mice, while the abundance of death-associated protein kinase (DAPK) and integrin linked kinase (ILK) is increased. Finally, cyclosporine treatment reduces significantly proteinuria in PHN rats, concomitantly with downregulation of c-mip abundance in podocytes. These results suggest that c-mip plays an active role in podocyte disorders of MN.

Introduction

Idiopathic membranous nephropathy (MN) is a glomerular disease of unknown etiology, commonly associated with nephrotic syndrome. It is histologically characterized by diffuse thickening of the capillary loop, which results from the formation of subepithelial immune deposits consisting of immunoglobulin G (predominantly IgG4), complement components and recently identified antigens.¹⁻⁴ MN remains a major cause of nephrotic syndrome in adults, with up to 40% of patients progressing toward end stage renal failure after 10 years.⁵ Researches into the molecular mechanisms underlying the pathogenesis of MN were focused many years ago on the identification of target antigens, which initiate the formation of the immune complex. The generation of an experimental model of MN established in rats by Heymann and coworkers fifty years ago, represents the start-point of pathophysiological researches on MN.⁶ Active (AHN) and passive type Heymann (PHN) nephritis were induced by direct immunization of Lewis rats with crude preparation of brush border proteins or by injection of rabbit anti-rat brush border antibodies, respectively. Both AHN and PHN closely mimic the human glomerular disease.⁷ The identification in this model of the target antigen, megalin, a common component of the tubular and glomerular epithelial cell provided the molecular basis of podocyte disease in MN.⁸ Nevertheless, since human podocytes do not express megalin, it cannot be considered as the target antigen in human MN.¹ In the last decades, many studies have focused on the identification of the antigen involved in human MN. Several antigens involved in secondary forms of MN caused by infectious disease and cancer have been found in subepithelial immune deposits, without clear evidence for a direct pathogenic role. The first identification of a pathogenic antigen in human MN came from Ronco's team who identified neutral endopeptidase (NEP) as the podocyte target of nephritogenic antibodies in patients with neonatal MN.^{10, 11} The anti-NEP antibodies resulted from immunization against the placental NEP of a NEP-deficient

1 mother. In this form of MN, the membrane attack of complement (C5b-9) was also detected
2 within the immune deposits, which indicated that like anti-megalin antibodies, anti-NEP could
3 induce complement activation potentially leading to podocyte injury.^{11, 12} Subsequently, Beck et
4 al reported that about 70% of patients with idiopathic MN have autoantibodies that react with the
5 M-type phospholipase A2 receptor (PLA2-R), a glycoprotein constitutively expressed in
6 podocytes.³ Prunotto et al. identified two additional targets of autoimmunity, aldoreductase and
7 SOD2, both induced in glomeruli of patients with MN.⁴

8 The onset of proteinuria during the course of MN is associated with phenotypic alteration of
9 podocyte and slit diaphragm integrity as demonstrated in a Heymann nephritis model.¹³⁻¹⁵ The
10 abundance of nephrin, a major protein of slit diaphragm, is reduced in PHN and in biopsies from
11 patients with MN, while the mRNA and protein expression of cation permeable ion channel
12 TRPC6, which is mutated in the familial form of focal segmental glomerulosclerosis,¹⁶ is
13 increased.^{13-15, 17, 18} However, the mechanisms that lead to these alterations remain partly
14 obscure

15 The membrane attack complex of complement C5b-9/Mac is thought to play a crucial role in the
16 induction of podocyte injury leading to proteinuria in this model.^{12, 19} In PHN, proteinuria has
17 been suggested to be entirely dependent on C5b-9/Mac.²⁰ These data have recently been
18 challenged by the finding that AHN and PHN can be induced in rat deficient in complement
19 component C6, which is unable to form Mac.^{21, 22} Indeed, in PVG/C6^{-/-} rats, the degree of
20 proteinuria, the extent of cellular infiltrates, the abundance of Ig, C3 and electron-dense deposits
21 were similar to those observed in the PVG/c rats.²² Anti-podocyte antibodies including anti-
22 megalin, anti-NEP and anti-PLA2-R are directed against functional receptor or enzymatic
23 proteins, so that their binding may induce a cascade of events that may directly alter podocyte
24 biology.²³

25 In the wake of studies aimed to understand the molecular pathophysiology of idiopathic
26 nephrotic syndrome, we identified a new gene, *c-mip* (for *c*-maf inducing protein), which
27 encodes an 86-kDa protein.²⁴ The predicted structure of *c-mip* includes an N-terminal region

1 containing a pleckstrin homology domain (PH), a middle region characterized by the presence of
2 several interacting docking sites including a 14-3-3 module, a PKC domain, an Erk domain, a
3 SH3 domain similar to the p85 regulatory subunit of phosphatidylinositol 3-kinase (PI3K), and a
4 C-terminal region containing a leucin-rich repeat (LRR) domain.
5
6
7
8

9 We have recently shown that c-mip abundance is increased in MN during relapse,²⁵ which
10 led us to study its potential implication in Heymann nephritis. We report here that c-mip protein
11 is not induced at the early stage of PHN, when the immune complex deposits are formed without
12 inducing proteinuria, but increases very quickly after a second injection of anti-megalin
13 polyclonal antibodies, while proteinuria concomitantly rises to reach nephrotic range. We
14 provide evidence that c-mip induces *in vivo* and *in vitro* podocyte dysfunctions that are common
15 to MN and PHN.
16
17
18
19
20
21
22
23
24
25
26
27
28
29
30
31
32
33
34
35
36
37
38
39
40
41
42
43
44
45
46
47
48
49
50
51
52
53
54
55
56
57
58
59
60

Results

Renal expression of c-mip in membranous nephropathy and passive Heymann Nephritis

Northern blot analysis showed that basal expression of *c-mip* in podocyte was scarcely or below the detection limits in control human kidneys ([Figure 1a](#)), which suggests that *c-mip* is transcriptionally repressed in physiological situations. However, quantitative PCR from laser microdissected glomeruli from five control samples and eleven MN biopsy specimens showed that *c-mip* abundance was significantly increased in MN ([Figure 1b](#)). In addition, we confirmed by *in situ* hybridization ([Figure 1c](#)), confocal immunofluorescence ([Figure 1d](#)) and immunohistochemistry analysis (supplementary Figure S1) that *c-mip* was overproduced at the mRNA and protein levels in patients with MN.

The finding that *c-mip* was highly induced in podocytes of patients with MN led us to study its expression in Heymann nephritis, the experimental model of human MN. We induced PHN by injection of anti-megalin polyclonal antibody. Proteinuria, as tested at day 13 post injection, was very slightly increased (urine protein to creatinine ratio, UPr/UCr, mg/mg \pm SD: 1.53 ± 0.20) relatively to controls (0.63 ± 0.057) ([Figure 2a](#)). At day 12, immunofluorescence analysis of kidney sections showed granular deposits of IgG along the glomerular capillary loops in rats with PHN, while no staining was visualized in control rats ([Figure 2b](#)). Following a second injection two weeks after the first one (day 14), rats developed heavy proteinuria that reached a peak at day 19 (UPr/UCr: 9.48 ± 7.64) ([Figure 2a](#)). Quantitative RT-PCR from laser microdissected glomeruli (n= 3 rats at each time point) showed that *c-mip* abundance was markedly increased 24 hours after the second immunization ([Figure 2c](#)). *C-mip* was visualized by immunohistochemistry by day 13 post-injection and increased much at day 15, whereas no signal was detected before ([Figure 2d](#)). Overproduction of *c-mip* persisted until day 42, along the experimental procedure. These results suggest that *c-mip* induction is paralleled to development of proteinuria.

Overexpression of c-mip induces phenotypical and biochemical alterations

To understand the effects of *c-mip* on podocyte function in PHN, we established stably transfected podocyte cell lines using the inducible T Rex system. Stable *c-mip*-overexpressing cells exhibited abnormal morphology with retraction of cell body, loss of stress fibers and were more susceptible to cell

1 detachment from collagen matrix, whereas podocytes cultured in the absence of tetracycline proliferate
2 normally and exhibited long intracellular bundles of actin filaments ([Figure 3a](#) and supplementary Figure
3 S2). The abundance of synaptopodin, a regulator of podocyte actin cytoskeleton reorganization, was
4 decreased ([Figure 3b](#)). Interestingly, the abundance of synaptopodin was reduced in MN glomeruli and in
5 c-mip transgenic mice ([Figure 3c](#)).
6
7
8
9
10

11 Because RhoA is required for actin stress fiber formation by interacting notably with synaptopodin,²⁶ we
12 investigated RhoA activity in stably c-mip-transfected cells. In the absence of tetracycline, RhoA activity
13 was increased in stably transfected podocytes ([Figure 4a](#)). However, tetracycline treatment was associated
14 with lower RhoA activity ([Figure 4a](#)), but has no effect on Cdc42 activity ([Figure 4b](#)), while c-mip was
15 clearly induced ([Figure 4c](#)). Tetracycline treatment did not seem to have any influence on RhoA activity
16 in wild-type podocytes ([Figure 4d](#)).
17
18
19
20
21
22
23
24

25 The observation that c-mip alters the adhesion of cultured podocytes to collagen matrix led us to
26 explore whether c-mip affects the abundance of integrin linked kinase (ILK), an adhesion-associated
27 kinase, whose upregulation was shown to cause podocyte detachment.^{27, 28} Low ILK expression was
28 found in non-induced podocytes, whereas following tetracycline treatment stable c-mip-overexpressing
29 cells exhibited increased ILK levels but podocin abundance did not significantly change ([Figure 5a](#)).
30 Because cell detachment from the extracellular matrix alters matrix-transduced survival pathways and
31 cytoskeleton architecture, resulting in release of proapoptotic factors,²⁹ we tested whether c-mip affects
32 the expression of death-associated protein kinase (DAPK), an actin filament-associated proapoptotic
33 protein.³⁰ Immunoblotting revealed that podocytes expressing c-mip exhibited higher abundance of
34 DAPK ([Figure 5a](#)). The relevance of these findings was tested *in vivo* both in transgenic mice and PHN
35 rats. Western blot analysis of glomerular lysates showed that c-mip transgenic mice exhibited an
36 increased abundance of DAPK and ILK in c-mip transgenic mice, without significantly change in
37 podocin expression ([Figure 5b](#)). Moreover, increased amounts of DAPK and ILK were detected in PHN
38 rats ([Figure 5c](#)). We extended this analysis in MN biopsies and control kidneys (n = 5 in each group).
39 Quantitative PCR analysis of laser-microdissected glomeruli showed that DAPK and ILK transcript levels
40 were significantly increased in MN when compared with controls (DAPK: 1.62 ± 0.12 versus 1.18 ± 0.06 ,
41
42
43
44
45
46
47
48
49
50
51
52
53
54
55
56
57
58
59
60

1 p<0.05; ILK 1.52 ± 0.13 versus 1.14 ± 0.14 , p<0.05) ([Figure 5d](#)). Immunohistochemistry analysis
2 suggests that abundance of both proteins was also increased with a more diffuse pattern for ILK ([Figure](#)
3 [5e](#)). Altogether, these results suggest that c-mip overexpression alters both integrin-mediated cell–matrix
4
5
6 interaction and the regulation of prosurvival signals.
7
8
9

10 **Cyclosporine therapy inhibits c-mip expression and reduces proteinuria in Heymann nephritis**

11 To assess the influence of cyclosporine in this model, PHN rats displaying nephrotic proteinuria were
12 separated in two groups: the one was treated intraperitoneally by cyclosporine at 20 mg/kg daily (CsA
13 group) from the day 21 post-first immunization, while the control group received the vehicle (sodium
14 chloride). Proteinuria was analyzed every three days, between day 21 and day 42. UPr/UCr decreased
15 significantly from the third day-post CsA and reached the nadir at day 38 ([Figure 6a](#)). In the absence of
16 CsA treatment, proteinuria also decreased over time but remained at nephrotic range in control rats.
17 Quantitative RT-PCR analysis showed that c-mip abundance was reduced by 50% at day 42, as compared
18 with control PHN rats ([Figure 6b](#)). Immunohistochemistry analysis showed that c-mip protein was clearly
19 reduced in CsA-treated rats ([Figure 6c](#)). The abundance of active RhoA was increased ([Figure 6d](#)),
20 whereas ILK and DAPK abundances were reduced in CsA-treated rats ([Figure 6e and 6f](#)). Confocal
21 microscopy analysis showed that nephrin and synaptopodin were mostly downregulated in PHN rats, but
22 restored upon CsA treatment ([Figure 7](#)).
23
24
25
26
27
28
29
30
31
32
33
34
35
36
37
38
39
40
41
42
43
44
45
46
47
48
49
50
51
52
53
54
55
56
57
58
59
60

Discussion

Primary MN defines podocyte disease in which alterations occur commonly in the absence of inflammatory lesions or cell infiltration. Immunofluorescence (IF) findings show typical immunoglobulin and complement deposits along the capillary loop.³¹ Although the pathogenesis remains incompletely elucidated, the underlying mechanism involves the generation of antibodies directed against intrinsic podocyte antigens and subsequent formation of subepithelial dense deposits leading to complement activation and glomerular injuries.^{1, 3}

In this study, we showed that: i) c-mip abundance is significantly increased in human MN; ii) c-mip protein is slightly and belatedly detectable after the first anti-megalin injection although immune complexes are fully formed; iii) c-mip abundance is strongly increased following a second immunization and precedes the occurrence of nephrotic-proteinuria; iv) stably overexpression of c-mip in podocytes reproduces several podocyte alterations such as those observed in human MN and PHN including downregulation of nephrin and synaptopodin;^{17, 32, 25} v) c-mip induction in MN, PHN and Tg mice is associated with upregulation of DAPK and ILK, and vi) CsA inhibits the expression of c-mip and significantly reduces proteinuria, whereas the abundance of ILK and DAPK is reduced.

The time course of c-mip expression in PHN is closely related to that of proteinuria occurrence. Although the immune complex deposits were clearly formed in glomeruli of PHN rats receiving a single dose of anti-megalin, they did not develop abnormal proteinuria. Conversely, rats receiving a second injection of anti-megalin antibody develop proteinuria in parallel with an overproduction of c-mip. This finding is supported by our mouse model in which targeted expression of c-mip in podocytes induces nephrotic proteinuria. These observations suggest that podocyte damage leading to nephrotic proteinuria in PHN is associated with c-mip induction. It is interesting to note that c-mip is not induced in nephrotic syndromes associated with diabetic nephropathy, HIV-associated nephropathy, or IgA nephropathy,²⁵ suggesting that c-mip is specifically induced in some primary podocyte diseases of immune origin. Irrespective of

1 the earliest aggression leading to MN, our results suggest that c-mip induction may act as a second, major
2 event resulting in podocyte dysfunction.
3

4 We have previously shown that c-mip interacts with Fyn, a member of the Src kinase protein family, and
5 prevents its interaction with nephrin, which results in the inhibition of nephrin phosphorylation. This
6 mechanism may explain the downregulation of nephrin phosphorylation found both in minimal change
7 nephrotic syndrome (MCNS) and in c-mip Tg mice.^{33, 25} Likewise, it has been reported that nephrin is
8 also hypophosphorylated in MN.³⁴
9

10 In MN and MCNS, the pattern of nephrin expression shifts from linear epithelial to granular
11 interpodocyte filtration slits with changes in cytoskeleton organization, such as seen in c-mip Tg mice.²⁵
12 The downregulation of nephrin expression results at least in part from its shedding from the cell surface
13 and its passage to the urinary space.³⁵
14

15 According to previous reports, the onset of proteinuria in PHN does not coincide with the formation of
16 immune complex deposits but with the complement activation-mediated podocyte damage.¹⁴ The
17 mechanism by which the membrane attack of complement (C5b-9) alters nephrin signaling and
18 disorganizes the actin cytoskeleton has not been elucidated. Our results showing a clear correlation
19 between c-mip abundance and the occurrence of nephrotic-range proteinuria, suggest that c-mip plays a
20 pivotal role in MN, inasmuch that c-mip reproduces biochemical alterations in Tg mice similar to those
21 observed in MN, in the absence of any complement or immunoglobulin deposits.²⁵
22

23 Actin cytoskeleton is a highly dynamic structure that plays a central role in the normal morphology of
24 podocytes and establishing a functional link with neighboring foot processes. We have shown that stable
25 overexpression of c-mip in an inducible system (T Rex) alters the morphological characteristics of
26 podocytes and downregulates synaptopodin expression. It has been well established that RhoA regulates
27 contractility and assembly of actin stress fibers and focal adhesions. We show here that c-mip inhibits
28 RhoA activity, in agreement with recent studies showing that synaptopodin regulates the stability of
29 RhoA and modulates actin polymerization activity.²⁶
30

31 Anti-proteinuric properties of CsA have been demonstrated both in patients with MN and in Heymann
32 nephritis^{36, 37}. According, we show that CsA reduces proteinuria in PHN, in parallel with downregulation
33
34
35
36
37
38
39
40
41
42
43
44
45
46
47
48
49
50
51
52
53
54
55
56
57
58
59
60

1 of c-mip and ILK. Although we cannot exclude that antiproteinuric effect could be due to its
2 immunosuppressive action, we found that CsA restores nephrin and synaptopodin abundances in the
3 podocytes. Because calcineurin promotes dephosphorylation of synaptopodin and its subsequent
4 degradation,³⁸ the antiproteinuric effect involves at least in part the preservation of synaptopodin by CsA,
5 a potent calcineurin inhibitor.
6
7
8
9
10

11 Overexpression of c-mip *in vitro* and *in vivo* is associated with an increased expression of ILK, a
12 serine/threonine protein kinase involved in the cellular control of integrin-mediated cell–matrix
13 interaction and cell phenotype regulation. ILK contributes to tightly control the interaction of the
14 podocyte cytoskeleton with the matrix components of the glomerular basement membrane (GBM), which
15 is crucial to maintain the complex capillary architecture against the highly transcapillary pressure
16 gradient. Effacement of foot processes and podocyte retraction suggest that molecules at the interface
17 between cytoskeleton and integrin matrix may play a crucial role in these processes. ILK expression is
18 increased in situations associated with an effacement of foot processes, independently of the causal
19 mechanisms, such as congenital nephrosis of Finnish type and adryamicin /puroptomycin models of
20 proteinuria.^{39, 28} This leads to consider that upregulation of ILK in response to podocyte damage might
21 serve to stabilize the adhesion of unharmed podocytes to GBM, through multiple interactions with
22 cytoskeletal partners.⁴⁰ This hypothesis is supported by the fact that ILK is an anti-apoptotic molecule, as
23 opposed to c-mip, which exhibits proapoptotic properties.⁴¹
24
25
26
27
28
29
30
31
32
33
34
35
36
37
38
39
40

41 In conclusion, this work reveals that c-mip is overproduced in PHN and in human MN. Functional
42 studies suggest that c-mip might play a crucial role in podocyte damage in MN. Overexpression of c-mip
43 *in vivo* reproduces the biochemical alterations observed in Heymann nephritis as well as in MN, including
44 increased expression ILK, DAPK, downregulation of synaptopodin and inhibition of RhoA activity and
45 alteration of nephrin expression. Taken together, these results suggest that c-mip is a key player in
46 podocyte diseases and may represent a “hot” therapeutic target.
47
48
49
50
51
52
53
54
55
56
57
58
59
60

Materials and Methods

Patients.

The cohort of adult patients analyzed in this study has been described in a previous report.²⁵ Normal renal samples were supplied by the department of pathology, from patients undergoing nephrectomy for polar kidney tumor. PBMC were purified through a Ficoll/Hypaque density gradient (Eurobio, France). All experiments were conducted with approval from the INSERM (Institut National de la Santé et de la Recherche Médicale) research ethics committee in accordance to international ethics codes and guidelines. The informed consent was obtained from all participants involved in this study.

Light microscopy studies and immunohistochemical analyses

In situ hybridization (ISH) experiments using c-mip riboprobes have been previously described.²⁵ For immunohistochemistry analysis, kidney samples were fixed for 16 hours in Dubosq Brazil, and subsequently dehydrated and embedded in paraffin. Antigen retrieval was performed by immersing the slides in boiling 0.01 M citrate buffer in a 500 W microwave oven for 15 min. The endogenous peroxidase activity was blocked with 0,3% H₂O₂ in methanol for 30 min. Slides were incubated with the blocking reagents consisting of the Avidin–biotin solution for 30 min and the normal blocking serum for 20 min. For detection of c-mip, the slides were incubated overnight with a polyclonal antibody at a final concentration of 15 mg/ml, then with a biotinylated secondary antibody. An avidin-biotinylated horseradish peroxidase complex (Vectastain ABC Reagent, Vector Laboratories; Burlingame, CA) and 3,3'-diaminobenzidine (Sigma Biochemicals; St Louis, MO) as a chromogen were applied for visualization of the immunoreaction. Slides were counterstained with hematoxylin. Omission of the primary antibody was considered as a negative control.

Immunofluorescence labeling was carried out on 4-mm thick cryostat sections of kidney tissue fixed in acetone for 10 min, air-dried for 30 min at room temperature, then incubated in PBS for 3 min and blocked in 1% BSA in PBS. The sections were incubated with the indicated antibodies for 1 hour at room

1 temperature, washed in PBS and incubated with Red Texas-conjugated secondary antibodies. Sections
2
3 were examined by fluorescence microscopy (Zeiss).
4
5
6

7 **Northern blots and stable transfections**

8
9 Total RNA was prepared from glomerular fractions isolated by graded sieving, using Rnaeasy kit
10 (Quiagen, France). Northern blots were performed as previously described (Sahali, 2002 #3714}, using
11 human kidney samples isolated from normal tissues of total nephrectomy for polar tumors. Briefly,
12 twenty µg of total RNA from kidney were loaded on each lane. The blot was hybridized with a [³²P]
13 dCTP-labeled 1200 bp cDNA c-mip probe, then with a 18S ribosomal RNA antisens oligonucleotide
14 probe. Conditionally immortalized mouse podocyte cell line is a gift of Peter Mundel.⁴² Generation of
15 stably transfected podocytes was performed as previously reported.²⁵
16
17
18
19
20
21
22
23
24
25
26

27 **Immunoprecipitation and Western blotting**

28
29 The primary antibodies used in this study include anti-ILK, anti-RhoA and anti-DAPK (Upstate Cell
30 signaling, USA), anti-synaptopodin and anti-nephrin (Progen Biotechnik GmbH, Germany), anti-actin
31 (Sigma, Aldrich, France), anti-sheep-IgG (Santa Cruz, Biotechnology, Inc, USA). The anti-podocin
32 antibody was a gift from Dr Corinne Antignac (Inserm U983, Necker Hospital, France). The anti-c-mip
33 polyclonal antibody was produced in rabbits immunized with acrylamide gel sections containing the c-
34 mip protein. Immunoprecipitation and Western blotting were performed as previously reported.²⁵
35
36
37
38
39
40
41
42
43
44

45 **RhoA and Cdc42 activation assays**

46
47 Activated RhoA and Cdc42 pull-down kits were purchased from Cytoskeleton (Cytoskeleton, Inc.,
48 Denver, USA) and the assays performed following supplied protocols. Briefly, stably transfected
49 podocytes were incubated without or with tetracycline (1 µg/ml) for 48 hours as previously described,
50 then cells were lysed for protein extraction. The protein concentration of lysates was determined by
51 Bradford reaction assay. Equal amount of protein lysates were incubated with Rhotekin-RBD (RhoA
52 assay) or PAK-PBD (Cdc42 assay) affinity beads for 1 hour at 4°C, followed by two washes in lysis
53
54
55
56
57
58
59
60

1 buffer and three washes in the supplied wash buffer. Bound proteins were eluted in 1x Laemmli buffer
2
3 and examined by 15% SDS-PAGE and western blot analysis.
4
5
6

7 **Induction of passive Heymann Nephritis**

8
9 PHN was induced in male Lewis rats weighting 100 g by intravenous injection of sheep anti-rat megalin
10 antiserum (kindly provided by Pr Pierre Verroust, INSERM U538, St Antoine Hospital). Two injections
11 at fifteen day's-interval were performed. Twenty rats were injected with anti-megalín antiserum and five
12 control rats received equal volume of normal sheep serum. Individual rats were housed in metabolic
13 cages (Techniplast, France). Urines were collected after 24 hours and this was repeated five times for
14 each individual. Proteinuria was performed using appropriate kits from Advia Chemistry 1650 (Bayer
15 Healthcare AG, Leverkusen, Germany). Rats were sacrificed between 15 and 28 days following the
16 second injection.
17
18
19
20
21
22
23
24
25
26
27
28

29 **Cyclosporine (CsA) treatment**

30
31 At day 21 post-first immunization, PHN rats with well established nephrotic proteinuria were separated
32 into two groups (n=5 each). The first one (CsA group) was treated with CsA (Sandimmun^R, Novartis)
33 by daily intraperitoneal injection of CsA (20 mg/kg body weight) until proteinuria decreased
34 significantly (Day 42). The second group (control) received intraperitoneal injection of an equal volume
35 of sodium chloride solution (NaCl 0,9%). At day 42, rats were sacrificed and kidneys were processed
36 for analysis.
37
38
39
40
41
42
43
44
45
46

47 **Laser capture microdissection, reverse transcription and real time quantitative PCR (RT-qPCR)**

48
49 Serial sections (25 µm-thick rat frozen tissue specimens) were placed on membrane slides (Carl Zeiss
50 MicroImaging). Cresyl violet staining was performed by using a protocol from Zeiss Labs, Munich,
51 Germany.⁴³ Glomerular structures were selectively dissected using the PALM MicroBeam system (Carl
52 Zeiss). Each rat kidney sample was entirely microdissected, giving around 500 glomeruli from which
53 RNAs were extracted in triplicate (about 170 glomeruli/tube) with PicoPureTM RNA Isolation Kit
54
55
56
57
58
59
60

(Arcturus, Applied Biosystem, USA)). For human kidney biopsy specimens from patients with membranous nephropathy, glomeruli were isolated as previously described.⁴⁴ A representative figure of human and rat glomeruli before and after laser microdissection is shown in supplementary material (Figure S2). Reverse transcription (RT) was performed with Maxima First Strand cDNA synthesis Kit (Fermentas). Real time quantitative polymerase chain reaction (qPCR) was performed using the oligonucleotides listed in Table 1. Samples (2 µl of the RT reaction mixture, corresponding to 10 ng of equivalent total RNA) were amplified in a 20 µl reaction mixture containing 0.5 mM levels of each primer and 1 X Quantitect Sybr Green PCR mix (QIAGEN GmbH, Hilden, Germany). PCR was performed in a Light Cycler 480 apparatus (Roche Diagnostic). The c-mip primers amplified a 176-bp sequence (Table 1). A standard curve was generated for qPCR by using serial dilutions of linearized pdonr221-c-mip plasmid. The copy number was calculated as described (<http://www.uri.edu/research/gsc/resources/cndna.html>). PCR was initiated by denaturation at 95°C for 15 min, followed by 32 three-step cycles (95°C for 10 s, 63°C for 30 s, and 72°C for 30 s). A dissociation run (95°C for 5 sec followed by 65°C for one min) was performed at the end of PCR program allowing the generation of melting curve. The relative value for each sample was calculated using LightCycler analysis software. All PCR data were normalized to 18S rRNA expression, to control for variations in RT reactions.

The PCR conditions for ILK and DAPK are shown in Table 1.

Generation of c-mip transgenic mice

The generation of c-mip transgenic mice has been previously described.²⁵ All experiments involving animals were conducted in accordance with French laws.

Statistics

The data presented are means ± SD and were prepared with GraphPad Prism software, version 4.0. Mann-Whitney test was used to evaluate the significance of differences. Values of $P < 0.05$ were considered significant.

References

1. Ronco P, Debiec H. Molecular pathomechanisms of membranous nephropathy: from Heymann nephritis to alloimmunization. *J Am Soc Nephrol* 2005; **16**: 1205-1213.
2. Imai H, Hamai K, Komatsuda A, *et al.* IgG subclasses in patients with membranoproliferative glomerulonephritis, membranous nephropathy, and lupus nephritis. *Kidney Int* 1997; **51**: 270-276.
3. Beck LH, Jr., Bonegio RG, Lambeau G, *et al.* M-type phospholipase A2 receptor as target antigen in idiopathic membranous nephropathy. *N Engl J Med* 2009; **361**: 11-21.
4. Prunotto M, Carnevali ML, Candiano G, *et al.* Autoimmunity in membranous nephropathy targets aldose reductase and SOD2. *J Am Soc Nephrol* **21**: 507-519.
5. Glasscock RJ. Diagnosis and natural course of membranous nephropathy. *Semin Nephrol* 2003; **23**: 324-332.
6. Heymann W, Hackel DB, Harwood S, *et al.* Production of nephrotic syndrome in rats by Freund's adjuvants and rat kidney suspensions. *Proc Soc Exp Biol Med* 1959; **100**: 660-664.
7. Ronco P, Debiec H. Target antigens and nephritogenic antibodies in membranous nephropathy: of rats and men. *Semin Immunopathol* 2007.
8. Kerjaschki D, Farquhar MG. The pathogenic antigen of Heymann nephritis is a membrane glycoprotein of the renal proximal tubule brush border. *Proc Natl Acad Sci U S A* 1982; **79**: 5557-5561.
9. Kerjaschki D, Farquhar MG. Immunocytochemical localization of the Heymann nephritis antigen (GP330) in glomerular epithelial cells of normal Lewis rats. *J Exp Med* 1983; **157**: 667-686.
10. Debiec H, Guignon V, Mougnot B, *et al.* Antenatal membranous glomerulonephritis due to anti-neutral endopeptidase antibodies. *N Engl J Med* 2002; **346**: 2053-2060.
11. Debiec H, Nauta J, Coulet F, *et al.* Role of truncating mutations in MME gene in fetomaternal alloimmunisation and antenatal glomerulopathies. *Lancet* 2004; **364**: 1252-1259.
12. Salant DJ, Belok S, Madaio MP, *et al.* A new role for complement in experimental membranous nephropathy in rats. *J Clin Invest* 1980; **66**: 1339-1350.
13. Yuan H, Takeuchi E, Taylor GA, *et al.* Nephritin dissociates from actin, and its expression is reduced in early experimental membranous nephropathy. *J Am Soc Nephrol* 2002; **13**: 946-956.
14. Saran AM, Yuan H, Takeuchi E, *et al.* Complement mediates nephritin redistribution and actin dissociation in experimental membranous nephropathy. *Kidney Int* 2003; **64**: 2072-2078.
15. Nakatsue T, Koike H, Han GD, *et al.* Nephritin and podocin dissociate at the onset of proteinuria in experimental membranous nephropathy. *Kidney Int* 2005; **67**: 2239-2253.
16. Reiser J, Polu KR, Moller CC, *et al.* TRPC6 is a glomerular slit diaphragm-associated channel required for normal renal function. *Nat Genet* 2005; **37**: 739-744.

17. Doublie S, Ruotsalainen V, Salvidio G, *et al.* Nephlin redistribution on podocytes is a potential mechanism for proteinuria in patients with primary acquired nephrotic syndrome. *Am J Pathol* 2001; **158**: 1723-1731.
18. Moller CC, Wei C, Altintas MM, *et al.* Induction of TRPC6 channel in acquired forms of proteinuric kidney disease. *J Am Soc Nephrol* 2007; **18**: 29-36.
19. Cunningham PN, Quigg RJ. Contrasting roles of complement activation and its regulation in membranous nephropathy. *J Am Soc Nephrol* 2005; **16**: 1214-1222.
20. Couser WG. Pathogenesis of glomerular damage in glomerulonephritis. *Nephrol Dial Transplant* 1998; **13**: 10-15.
21. Leenaerts PL, Hall BM, Van Damme BJ, *et al.* Active Heymann nephritis in complement component C6 deficient rats. *Kidney Int* 1995; **47**: 1604-1614.
22. Spicer ST, Tran GT, Killingsworth MC, *et al.* Induction of passive Heymann nephritis in complement component 6-deficient PVG rats. *J Immunol* 2007; **179**: 172-178.
23. Ronco P, Debiec H. Antigen identification in membranous nephropathy moves toward targeted monitoring and new therapy. *J Am Soc Nephrol* 2010; **21**: 564-569.
24. Sahali D, Pawlak A, Valanciute A, *et al.* A novel approach to investigation of the pathogenesis of active minimal- change nephrotic syndrome using subtracted cDNA library screening. *J Am Soc Nephrol* 2002; **13**: 1238-1247.
25. Zhang SY, Kamal M, Dahan K, *et al.* c-mip impairs podocyte proximal signaling and induces heavy proteinuria. *Sci Signal* 2010; **3**: ra39.
26. Asanuma K, Yanagida-Asanuma E, Faul C, *et al.* Synaptopodin orchestrates actin organization and cell motility via regulation of RhoA signalling. *Nat Cell Biol* 2006; **8**: 485-491.
27. Hannigan GE, Leung-Hagesteijn C, Fitz-Gibbon L, *et al.* Regulation of cell adhesion and anchorage-dependent growth by a new beta 1-integrin-linked protein kinase. *Nature* 1996; **379**: 91-96.
28. Teixeira Vde P, Blattner SM, Li M, *et al.* Functional consequences of integrin-linked kinase activation in podocyte damage. *Kidney Int* 2005; **67**: 514-523.
29. Puthalakath H, Huang DC, O'Reilly LA, *et al.* The proapoptotic activity of the Bcl-2 family member Bim is regulated by interaction with the dynein motor complex. *Mol Cell* 1999; **3**: 287-296.
30. Wang WJ, Kuo JC, Yao CC, *et al.* DAP-kinase induces apoptosis by suppressing integrin activity and disrupting matrix survival signals. *J Cell Biol* 2002; **159**: 169-179.
31. Wiggins RC. The spectrum of podocytopathies: a unifying view of glomerular diseases. *Kidney Int* 2007; **71**: 1205-1214.
32. Honkanen E, von Willebrand E, Koskinen P, *et al.* Decreased expression of vascular endothelial growth factor in idiopathic membranous glomerulonephritis: relationships to clinical course. *Am J Kidney Dis* 2003; **42**: 1139-1148.

- 1
2
3
4
5
6
7
8
9
10
11
12
13
14
15
16
17
18
19
20
21
22
23
24
25
26
27
28
29
30
31
32
33
34
35
36
37
38
39
40
41
42
43
44
45
46
47
48
49
50
51
52
53
54
55
56
57
58
59
60
33. Uchida K, Suzuki K, Iwamoto M, *et al.* Decreased tyrosine phosphorylation of nephrin in rat and human nephrosis. *Kidney Int* 2008.
 34. Ohashi T, Uchida K, Asamiya Y, *et al.* Phosphorylation status of nephrin in human membranous nephropathy. *Clin Exp Nephrol* **14**: 51-55.
 35. Yu D, Petermann A, Kunter U, *et al.* Urinary podocyte loss is a more specific marker of ongoing glomerular damage than proteinuria. *J Am Soc Nephrol* 2005; **16**: 1733-1741.
 36. Ambalavanan S, Fauvel JP, Sibley RK, *et al.* Mechanism of the antiproteinuric effect of cyclosporine in membranous nephropathy. *J Am Soc Nephrol* 1996; **7**: 290-298.
 37. Blume C, Heise G, Hess A, *et al.* Different effect of cyclosporine A and mycophenolate mofetil on passive Heymann nephritis in the rat. *Nephron Exp Nephrol* 2005; **100**: e104-112.
 38. Faul C, Donnelly M, Merscher-Gomez S, *et al.* The actin cytoskeleton of kidney podocytes is a direct target of the antiproteinuric effect of cyclosporine A. *Nat Med* 2008; **14**: 931-938.
 39. Kretzler M, Teixeira VP, Unschuld PG, *et al.* Integrin-linked kinase as a candidate downstream effector in proteinuria. *Faseb J* 2001; **15**: 1843-1845.
 40. Wu C, Dedhar S. Integrin-linked kinase (ILK) and its interactors: a new paradigm for the coupling of extracellular matrix to actin cytoskeleton and signaling complexes. *J Cell Biol* 2001; **155**: 505-510.
 41. Ory, V, Fan, Q, Hamdaoui, N, Zhang, SY, Desvaux, D, Audard, V, Candelier, M, Noel, LH, Lang, P, Guellaen, G, Pawlak, A, Sahali, D: c-mip Down-Regulates NF-kappaB Activity and Promotes Apoptosis in Podocytes. *Am J Pathol*, 180: 2284-2292, 2012.
 42. Mundel P, Reiser J, Zuniga Mejia Borja A, *et al.* Rearrangements of the cytoskeleton and cell contacts induce process formation during differentiation of conditionally immortalized mouse podocyte cell lines. *Exp Cell Res* 1997; **236**: 248-258.
 43. Aaltonen KE, Ebbesson A, Wigerup C, *et al.* Laser capture microdissection (LCM) and whole genome amplification (WGA) of DNA from normal breast tissue --- optimization for genome wide array analyses. *BMC Res Notes* 2011; **4**: 69.
 44. Audard V, Zhang SY, Copie-Bergman C, *et al.* Occurrence of minimal change nephrotic syndrome in classical Hodgkin lymphoma is closely related to the induction of c-mip in Hodgkin-Reed Sternberg cells and podocytes. *Blood* 2010; **115**: 3756-3762.

Legends

Figure 1. c-mip abundance is significantly increased in membranous nephropathy (MN).

(a) Northern Blot analysis of c-mip expression in control kidneys. Twenty μg of total RNA from kidney were loaded on each lane. The blot was hybridized with a [^{32}P] dCTP-labeled 1200 bp cDNA cmip probe, then with a 18S ribosomal RNA antisens oligonucleotide probe. Positive control consists of total RNA from PBMC of a patient with MCNS relapse (Rel). The remission sample (Rem) from the same patient was included as internal control. (b) Quantitative RT-PCR of laser microdissected glomeruli from MN kidney biopsy specimens (n=11) and control kidneys (n=5). Relative copy numbers were calculated as described in Material and Methods. Mann-Whitney test, ** P <0.01. (c) In situ hybridization with a c-mip probe on control human kidney (NHK: normal human kidney) and kidney biopsy specimens from patients with MN (ASP: antisens probe; SP: sens probe). (d) Confocal double immunofluorescence labeling c-mip-nephrin on kidney biopsy specimens from patients with MN and control human kidney. Scale bars, 20 μm .

Figure 2. Induction of passive Heymann's nephritis (PHN).

Rat were injected with anti-megalin polyclonal antibody at two week's interval. (a), left, Urine samples (5 μl) and BSA (10 μg) were resolved by SDS-PAGE and gels stained with Coomassie Blue; right, proteinuria was assessed by calculating the proteinuria/urine creatinine ratio [UPr (mg)/UCr (mg)]. Data are expressed as means \pm SD. (b) Immunofluorescence detection of immune complex deposits using anti-sheep IgG in rats injected with anti-megalin antibody (day 12 after the first injection) and in control rats. (c) Quantitative RT-PCR of laser microdissected glomeruli from PHN (n=3 rats in each time point) and control rats (n=5). Relative copy numbers were calculated as described in Material and Methods. Mann-Whitney test, * P <0.05. (d) Immunodetection of c-mip in PHN. Representative immunohistochemical analysis of serial kidney sections from PHN and control rats. C-mip (brown signal) is detected along the external side of the capillary loop in PHN with higher abundance following reimmunization with sheep anti-megalin

1 polyclonal antibody. Scale bars, 20 μ m.
2
3
4

5 **Figure 3. Stable overexpression of c-mip in podocytes induces phenotypic and biochemical**

6 **alterations. (a)** Confocal microscopy analysis of phalloidin staining in stable transfectant murine
7 podocytes without [Tet(-)] and after induction of c-mip by tetracycline [Tet(+)]. *c-mip*-overexpressing
8 podocytes display a loss of stress fibers, whereas the actin network is well preserved in non-induced
9 stable transfectant cells. Scale bars, 20 μ M. **(b)** Western-blotting of protein lysates from non-induced
10 [Tet(-)] and induced [Tet(+)] *c-mip* stable transfectants. Overexpression of *c-mip* induces a
11 downregulation of synaptopodin. **(c)** Downregulation of synaptopodin in membranous nephropathy (MN)
12 and transgenic mice (Tg). Confocal microscopy analysis of synaptopodin on control human kidney (Con),
13 kidney biopsy specimens from patients with MN, wild type (wt) and *c-mip* Tg mice. Scale bars, 20 μ M.
14
15
16
17
18
19
20
21
22
23
24
25
26
27

28 **Figure 4. Stable overexpression of c-mip in podocytes inhibits RhoA activity but has no effect on**

29 **Cdc42 activity.** RhoA **(a)** and Cdc42 **(b)** activities were measured in stable transfectant podocytes
30 cultured in the absence [Tet(-)] or in the presence of tetracycline [Tet(+)] as indicated in the Material and
31 Method section. Nc: negative control; Pc Positive control. **(c)** Induction of *c-mip* by tetracycline in stable
32 transfectant podocytes. **(d)** Tetracycline has no influence on RhoA activity in wild-type podocytes.
33
34
35
36
37
38
39
40

41 **Figure 5. c-mip induces *in vitro* and *in vivo* an upregulation of ILK and DAPK. (a)** Representative

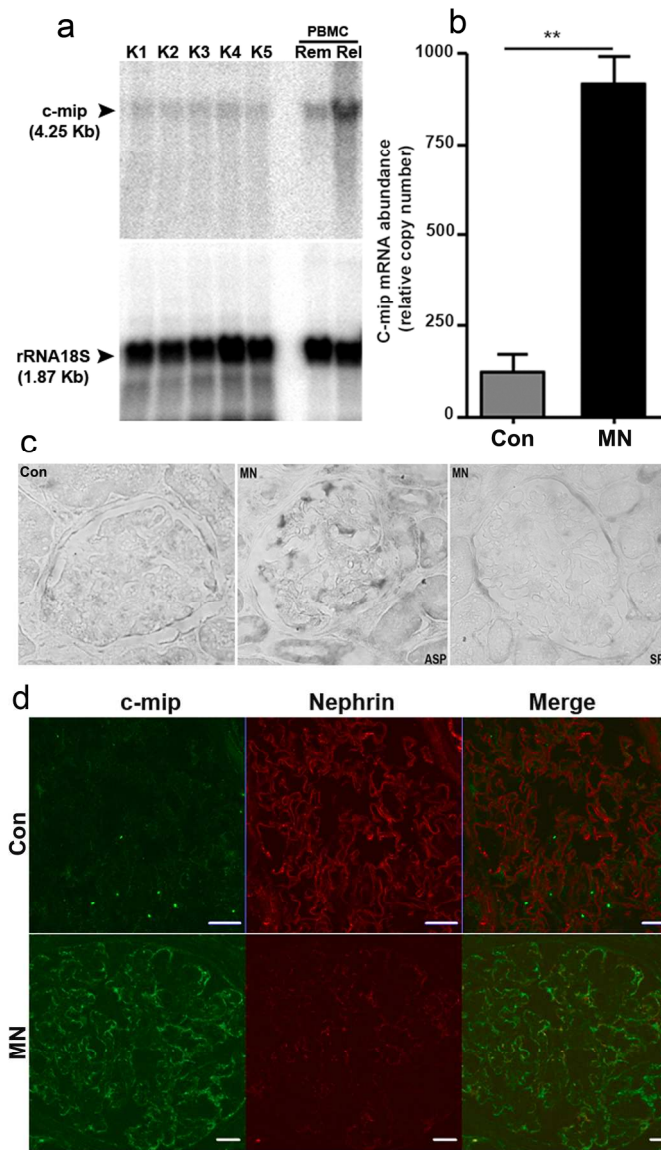
42 Western blots of ILK, podocin, *c-mip* and DAPK on protein lysates from non-induced [Tet(-)] and
43 induced [Tet(+)] stable transfectant podocytes. **(b)** Representative Western blots of DAPK and ILK on
44 glomerular lysates from wild-type and transgenic mice. **(c)** Representative Western blots of DAPK and
45 ILK on glomerular lysates from PHN and control rat kidneys (Con). **(d)** Quantitative RT-PCR of laser
46 microdissected glomeruli from MN kidney biopsy specimens (n=5) and control kidneys (n=5); * P <0.05,
47 Mann-Whitney test. **(e)** Representative immunohistochemical analysis of DAPK and ILK in serial
48 sections of kidney biopsy specimens from patients with MN and control human kidney (Con). Scale bars,
49 20 μ M
50
51
52
53
54
55
56
57
58
59
60

1
2
3 **Figure 6. Cyclosporine therapy inhibits c-mip expression and reduces proteinuria in PHN rats. (a)**
4
5 Course of proteinuria during CsA therapy started from the day 21 post-first immunization. left, Urine
6
7 samples (5 μ l) and BSA (10 μ g) were resolved by SDS-PAGE and gels stained with Coomassie Blue;
8
9 right, course of proteinuria as assessed by calculating the proteinuria/urine creatinine ratio (UPr/UCr). **(b)**
10
11 Quantitative RT-PCR of laser microdissected glomeruli from untreated [CsA(-)] and CsA-treated
12
13 [CsA(+)] PHN rats (n=5 rats in each group). Relative copy numbers were calculated as described in
14
15 Material and Methods; ** P <0.01, Mann-Whitney test. **(c)** Representative immunohistochemical analysis
16
17 for c-mip in serial kidney sections from CsA(-) and CsA(+) PHN rats (day 42 post-immunization). Scale
18
19 bars, 20 μ m. **(d-f)** Western blotting of RhoA, ILK and DAPK on glomerular lysates from CsA(-) and
20
21 CsA(+) PHN and control rats (Con), respectively.
22
23
24
25
26
27

28 **Figure 7. Confocal immunofluorescence labeling of nephrin, podocin and synaptopodin in kidney**
29
30 sections of CsA(-) and CsA(+) PHN rats (both at day 42 post-immunization) and control rats (Con). Scale
31
32 bars, 20 μ m.
33
34
35
36
37
38
39
40
41
42
43
44
45
46
47
48
49
50
51
52
53
54
55
56
57
58
59
60

Acknowledgments

We are grateful to Dr Peter Mundel for providing us with the mouse podocyte cell line and to Dr Corinne Antignac (INSERM U574, Hôpital Necker Enfant-Malades, Paris, France) for the gift of the anti-podocin antibody. We thank Dr Esmilaire Liliane (Biochemistry department, Henri Mondor Hospital) for biochemical dosages. We thank Dr Yves Allory (Pathology department) for providing us with renal samples. This work was supported in part by an Avenir Program from INSERM, a grant from the French Kidney Foundation and Association pour l'Utilisation du Rein Artificiel (AURA). V Audard is a recipient of a poste d'accueil INSERM. K Sendeyo was supported by grants of Ministère de la recherche et de la Technologie (MRT).



149x264mm (300 x 300 DPI)

1
2
3
4
5
6
7
8
9
10
11
12
13
14
15
16
17
18
19
20
21
22
23
24
25
26
27
28
29
30
31
32
33
34
35
36
37
38
39
40
41
42
43
44
45
46
47
48
49
50
51
52
53
54
55
56
57
58
59
60

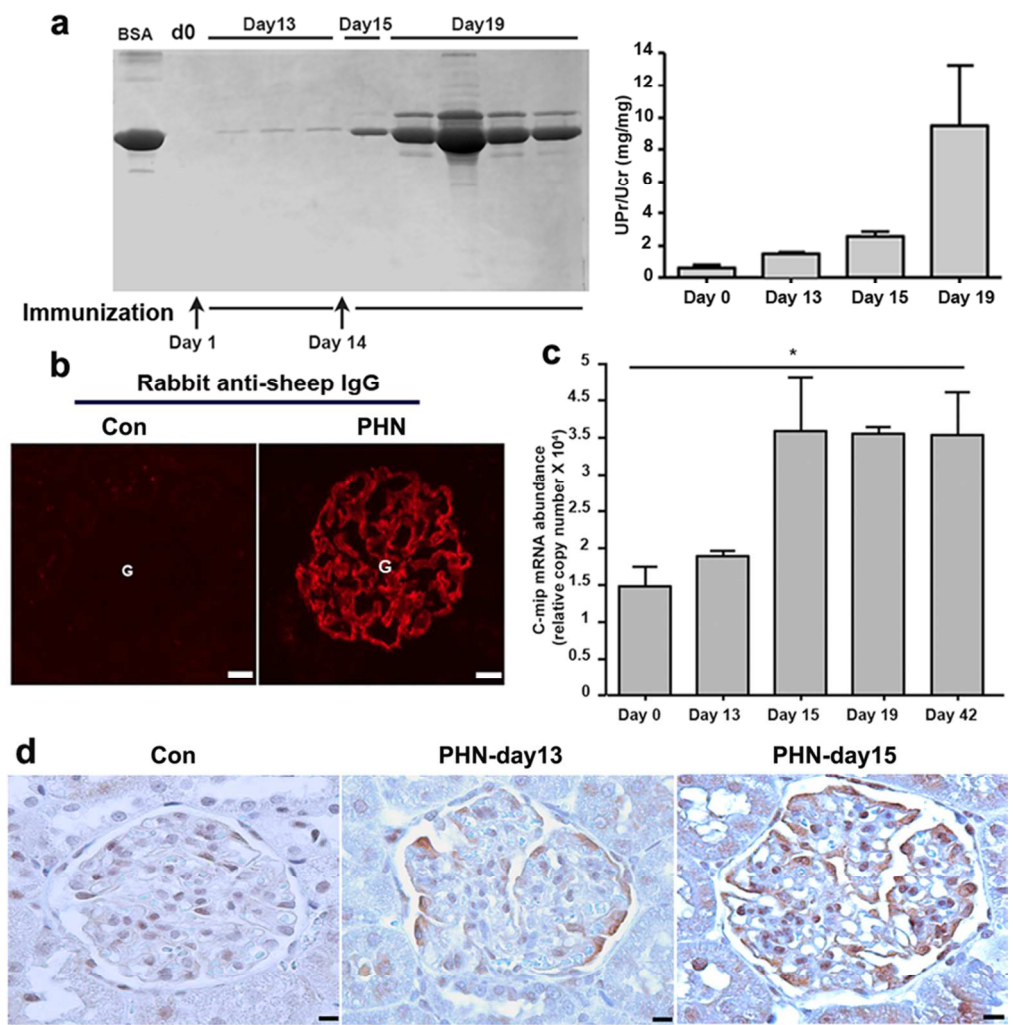


Fig. 2

86x93mm (300 x 300 DPI)



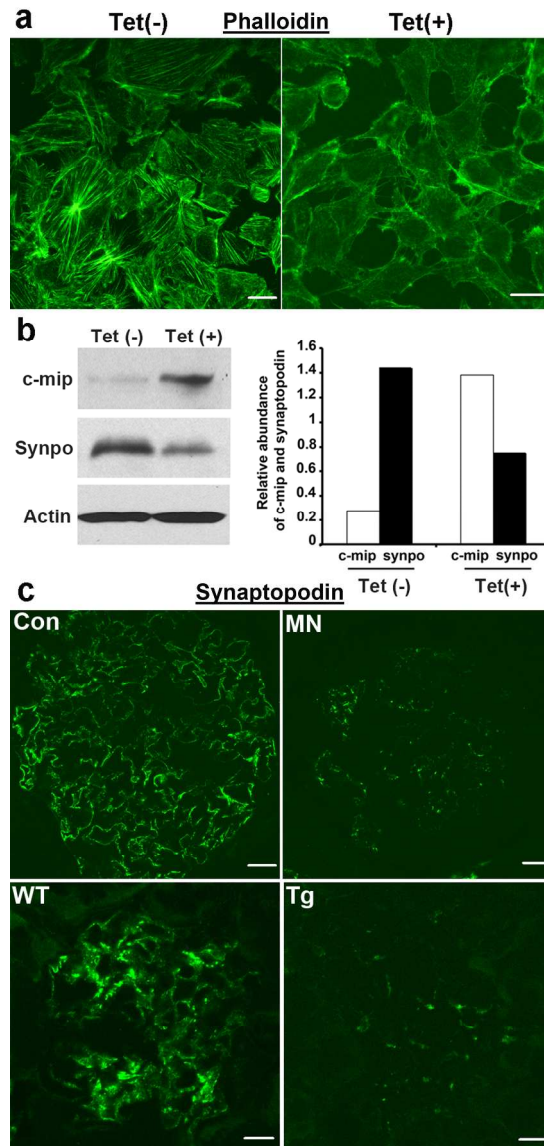


Fig.3

189x419mm (300 x 300 DPI)

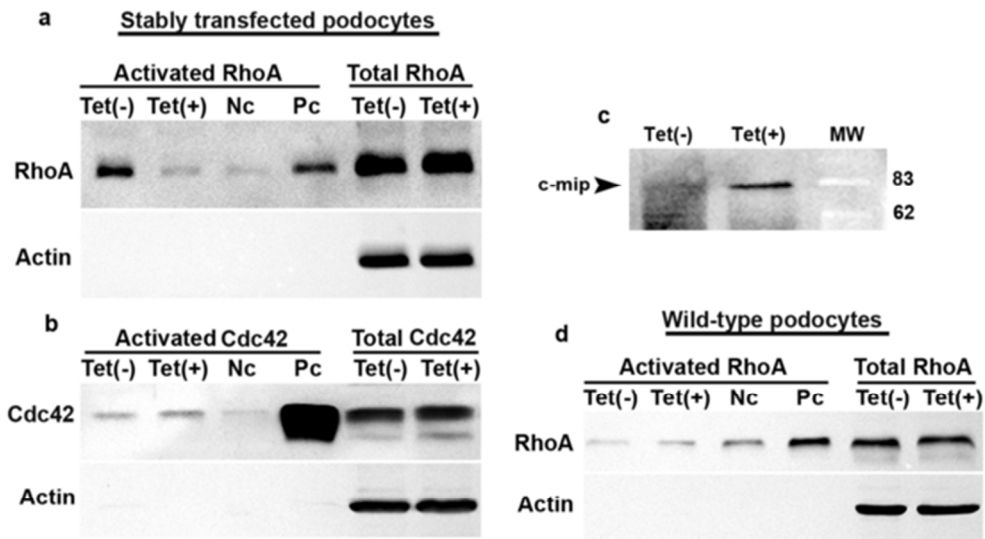
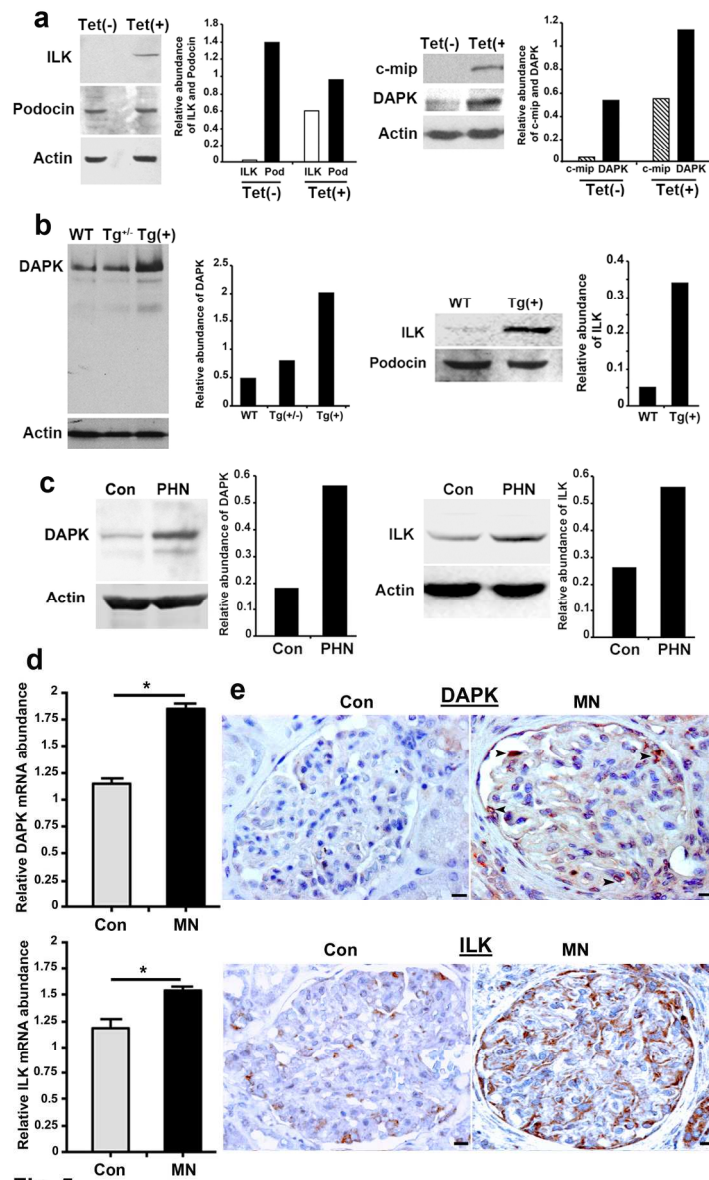


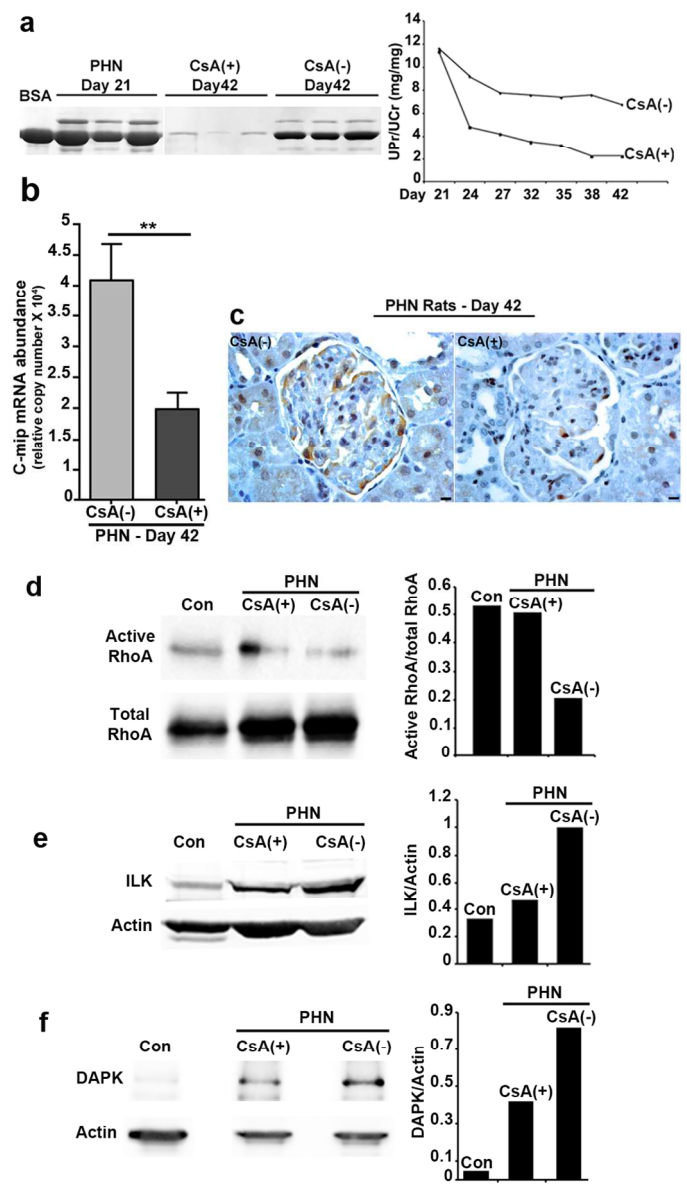
Fig. 4

53x33mm (300 x 300 DPI)

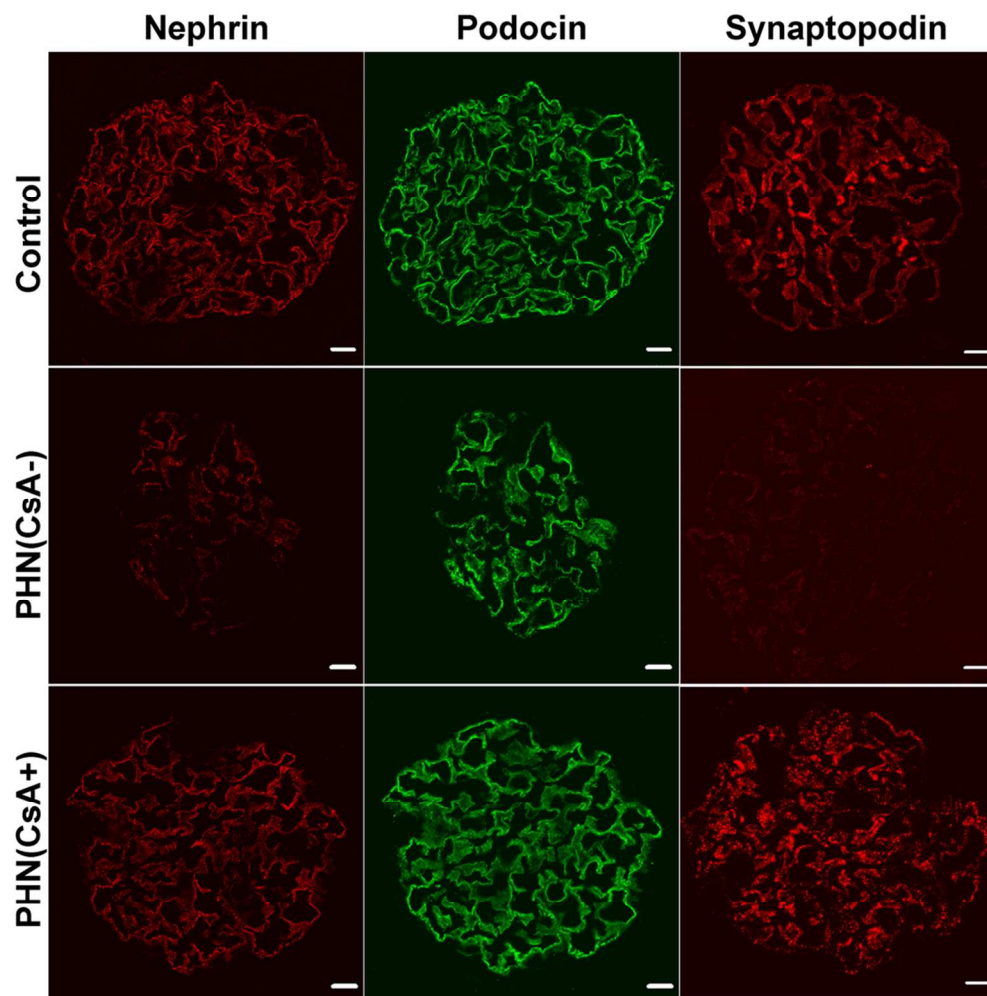


144x244mm (300 x 300 DPI)

1
2
3
4
5
6
7
8
9
10
11
12
13
14
15
16
17
18
19
20
21
22
23
24
25
26
27
28
29
30
31
32
33
34
35
36
37
38
39
40
41
42
43
44
45
46
47
48
49
50
51
52
53
54
55
56
57
58
59
60



85x152mm (300 x 300 DPI)

**Fig. 7**

94x104mm (300 x 300 DPI)



Table 1. Sequence of primers and PCR conditions.

Primers	Sequence	Accession number	Expected size	Ann Temp (°C)	PCR cycles
Rat c-mip	Forward: TGTGTGCCTGGCTGCCATATATTCTGCTATG	NM_001163273.1	176	64	32
	Reverse: GACAATGTGGCTTCCTGAGACACCAGGTC				
	18S	NR_003278	151	60	16
	Forward: GTAACCCGTTGAACCCATT				
	Reverse: CCATCCAATCGGTAGTAGCG				
Human c-mip	Forward: CGTGTGCCTGGCTGCCATCTACTCCTGCTATG	NM_198390	176	68	32
	Reverse: GACAGCGTGGCTTCCTGAGACACCAGGTC				
Human DAPK	Forward: CTCAGGCGCATTGCTCAGCAGCTC	NM_004938	248		
	Reverse: GATGTCCATGGCATCGAGGATCTGC				
Human ILK	Forward: GCAACGCAGTCGCCGTTTCGCCT	NM_001014795	210	58	35
	Forward: CACGGTGTCCATGACTGGCTGCCA				

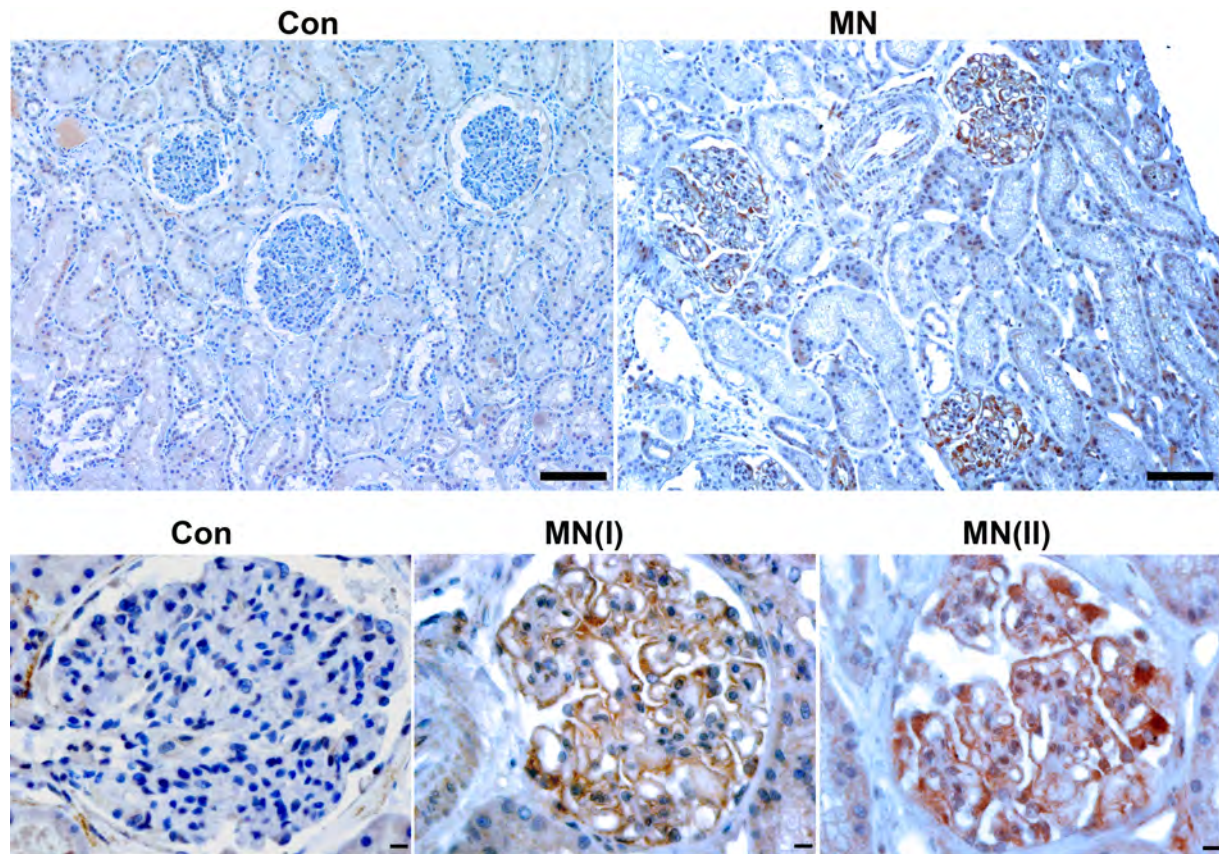


Figure S1: Representative immunohistochemical analysis of c-mip in serial sections of kidney biopsy specimens from patients with MN and control human kidney (Con). Scale bars, top panel 50 μ M; lower panel, 20 μ M

1
2
3
4
5
6
7
8
9
10
11
12
13
14
15
16
17
18
19
20
21
22
23
24
25
26
27
28
29
30
31
32
33
34
35
36
37
38
39
40
41
42
43
44
45
46
47
48
49
50
51
52
53
54
55
56
57
58
59
60

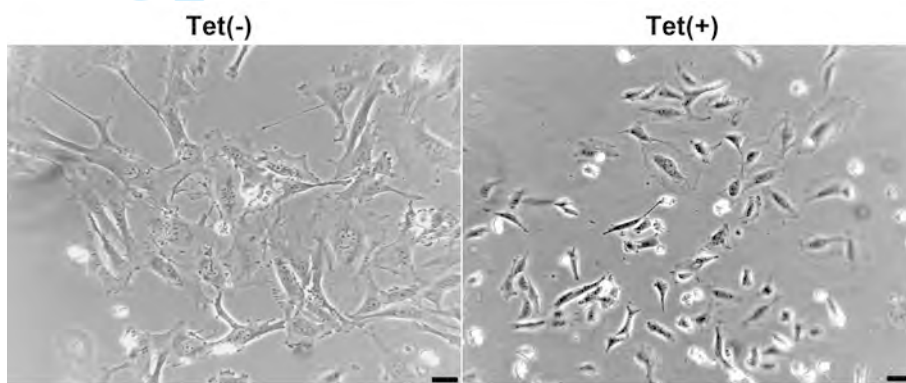


Figure S2: Stable overexpression of c-mip in podocytes induces phenotypic alterations. Light microscopy analysis of stable transfectant murine podocytes without [Tet(-)] and after induction of c-mip by tetracycline [Tet(+)].

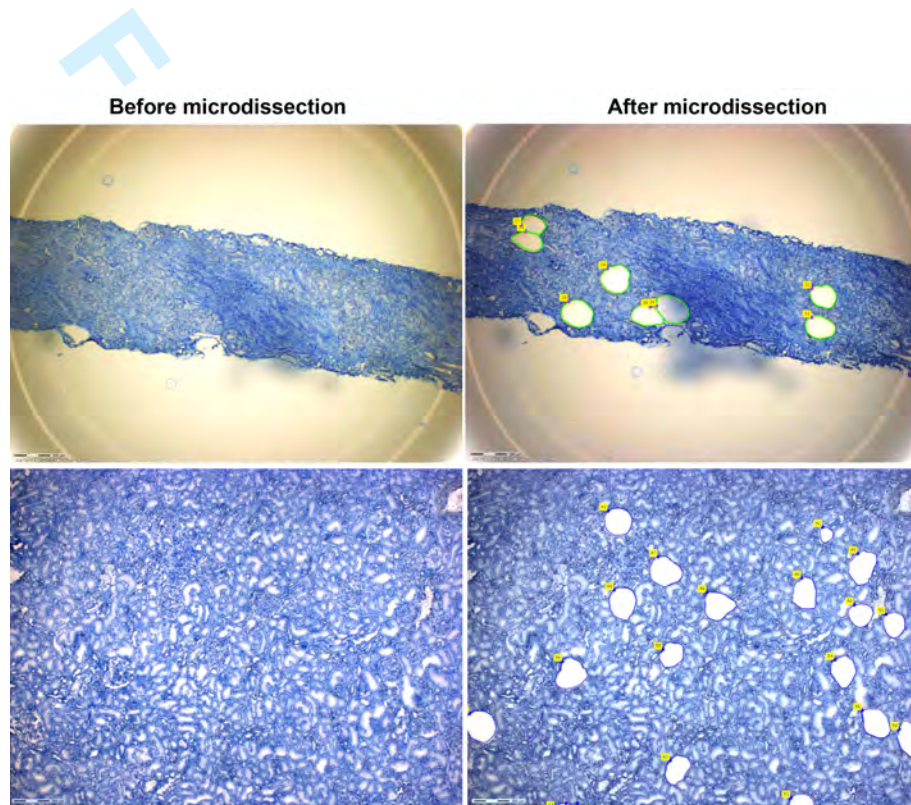


Figure S3: Micrographs of MN kidney biopsy specimens (top panel) and control human kidney (lower panel), before and after laser microdissection of glomeruli